euspen's 24th International Conference & Exhibition, Dublin, IE, June 2024
www.euspen.eu

Evaluation of the print geometry limitations of 3D printed continuous stainless steel fibre reinforced polymer composites

Alison Clarke[1], Vladimir Milosavljievic[2], Andrew Dickson[1] & Denis P. Dowling

[1]I-Form Centre, School of Mechanical and Materials Engineering, University College Dublin, Dublin, D04 V1W8, Belfield, Ireland
[2]Technological University Dublin, Park House, 191 N Circular Rd, Grangegorman, Dublin 7, D07 EWV, Ireland

alison.clarke1@ucdconnect.ie

Abstract

This study investigates the geometrical limitations of 3D printing continuous stainless steel fibre reinforced polymer composites. The printing study was carried out using a 316L stainless steel fibre (SSF) bundle with an approximate diameter of 0.15 mm. This bundle is composed of 90 fibres with a 14 μm diameter. This fibre bundle was firstly coated with polylactic acid (PLA), in order to produce the polymer coated continuous stainless steel filament, with diameters tailored in the range of 0.5 to 0.9 mm. These filaments were then used to print composite parts using the material extrusion (MEX) technique. To evaluate the geometry limitations of the printed polymer-SSF composites a series of prints were carried out through which print filament cornering and turning, a selection of angles and semi-circle radii were investigated. This investigation included printed part angles between 5 to 90°, along with semi-circles, with radii diameters between 2 and 20 mm, resulting in a series of 'teardrop' shaped geometries.

3D printing, stainless steel fibre, polylactic acid, curvature bending stiffness

1. Introduction

One of the most widely used 3D printing techniques is material extrusion (MEX) [1], [2]. Polymer composites are fabricated through the addition of fibres (short or continuous), alternatively powder particles, beads, and pellets [1], [3]–[6]. Reinforcing fibres available for MEX printed composite reinforcing fibres include glass, metal, carbon, and basalt [7]–[9]. The most commonly used thermoplastic feedstocks include Polylactic acid (PLA), Polycarbonate (PC), Polyamide (PA or nylon), and Acrylonitrile butadiene styrene (ABS) [1], [2], [4]–[6], [10].

The addition of particle and fibre reinforcing can substantially enhance the mechanical properties of 3D printed polymers. For example, PLA reinforced with continuous carbon fibre (PLA-CCF) was investigated by Li et al. [11]. The continuous carbon fibre bundle used contains up to a maximum of 1000 individual fibres. The resulting composite had a fibre volume fraction (Vf) of 34%, along with a tensile strength of up to 91 MPa. Nylon reinforced with continuous fibres of Kevlar, glass, and carbon, supplied by Markforged. The interlaminar shear strength was evaluated for Nylon-Kevlar, Nylon-glass, and Nylon-CF, with resultant strengths of 14.3, 21.0 and 31.9 MPa, respectively. Fibre content plays an important role in determining the properties of MEX composite filaments, with, for example, tensile strength generally increasing with increasing fibre content [1]. A difficulty, however, is that composite filaments, with high fibre content, can be very difficult to print, arising from issues with nozzle clogging, in addition to the excessive viscosity of the melted composite filament [10], [12]–[17].

In a previous study by the current authors filaments of continuous stainless steel fibre bundles within a polylactic acid (PLA) polymer were fabricated using a laboratory scale extrusion system [18]. By systematically controlling the 3D printing conditions, along with the use of a novel polymer pressure vent within the printer nozzle, 3D printed composites with fibre volume fractions between 4 and 30% were achieved. Good impregnation and adhesion of the PLA matrix into the stainless steel fibre were found based on an x-ray micro Computed Tomography (µCT) analysis, with the porosity of the resulting composites being in the range of 2 to 21%. The interlaminar shear strength ($\tau ILSS$) of the PLA-SSF with a volume fraction of 30% is found to be 28.5 MPa (±2.0), which is six times that of PLA only parts. Both the interlaminar shear strength and tensile strength properties of the composites were found to increase significantly as the stainless steel volume fraction (Vf) increased from 6 to 30%. The PLA-SSF composites exhibited tensile strengths of up to 249.8 MPa (±13.5), along with tensile modulus values of 14.3 GPa (±1.2). In the literature, the tensile strengths obtained with the highest stainless steel Vf in this study, are approximately four times higher than those reported for other printed metal fibre reinforced composites.

The objective of the current study is to evaluate the geometry limitations in the printing of continuous polymer-SSF parts. The study was carried out by varying the print geometries with part angles, between 5 to 90°, and semi-circles, with radii ranging from 2 to 20 mm.

2. Materials and methods

2.1. Materials and processing parameters

A continuous 316L stainless steel fibre (SSF) bundle was obtained from NV Bekaert SA (Belgium)[19]. The fabrication of a PLA - SSF filament was carried out from this steel fibre using a 3devo, laboratory-scale filament maker [20]. This was modified, to facilitate the introduction of the fibre into the molten polymer during filament extrusion as described previously [18]. The resulting PLA-SSF filaments were then used for the 3D printing of composite parts using a modified Anycubic i3 Mega polymer

extrusion printer as described previously [18]. To evaluate the continuous polymer-SSF materials' printability and geometrical limitations throughout cornering and turning, a selection of angles and semi-circle radii were investigated. The combination of angles, between 5 to 90°, and semi-circles, with radii ranging from 2 to 20mm, results in a series of 'teardrop' shaped geometries, as shown in Fig. 1.

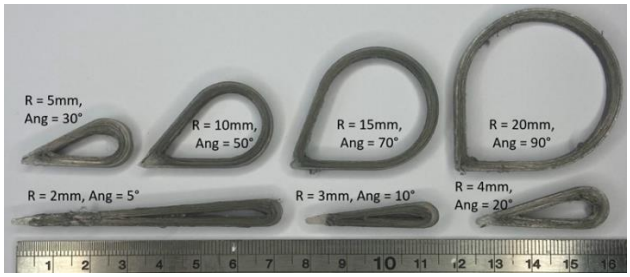

Figure 1. PLA-SSF 3D printed teardrop geometries

2.2. Composite characterisation

After printing the PLA-SSF teardrop composites (Figure 1), their dimensions, internal structure and morphology were examined. This evaluation was carried out by µCT scanning software VG studios, digital callipers and Dinolight microscope combined with a lighting box. The as-printed teardrop measurements are recorded and compared to the design dimensions. Measurements collection points are repeated on each sample by mapping and coding each geometry position.

Complementing the teardrop print study, an adaptation of the curve bend stiffness test standard ISO 14125, is used to determine the stiffness of the stainless steel reinforced composite as illustrated in Figure 2 [21]. The study investigated radii from 2 to 20 mm, with a minimum of five samples tested from each radius of 2, 3, 4, 5, 10, 15 and 20 mm. Along with testing the PLA-SSF semi-circles radii, neat PLA, Markforged Onex (Nylon – short carbon fibre) and Onex reinforced with continuous carbon fibre (Onex-cCF) were also printed with the same dimensions for comparison stiffness performance.

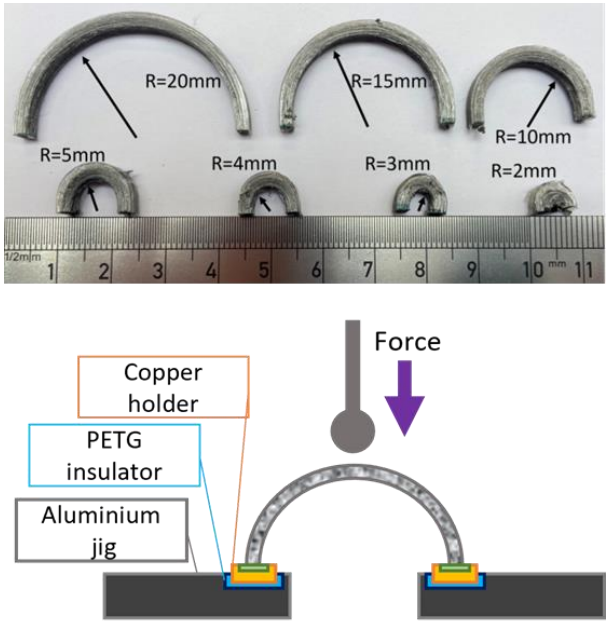

Figure 2: Curvature stiffness testing (CST), with a photograph of the PLA-SSF semi-circle test samples with radii as indicated (Top) and schematic of the test apparatus (Bottom)

The composite volume fraction and porosity are examined and evaluated using an X-ray µCT scanner, using ImageJ to cross-reference scanning electron microscope (SEM) and microscope cross-sections. The PLA-SSF tensile and ILSS samples resulted in a volume fraction of 30 V_f%. Where the teardrop and semi-circles in the range of 20-25 V_f%, this variation is due to the excess polymer surrounding the SSF and measurement position in the structure. All components result in a porosity of approximately 2%.

The PLA-SSF teardrop internal structure, morphology and dimensions are investigated by µCT scanning software VG studios, digital callipers and Dinolight microscope combined with a lighting box. The as-printed teardrop measurements are recorded and compared to the design dimensions. Measurements collection points are repeated on each sample by mapping and coding each position.

3. Results and discussion

The objective of this study is to evaluate the geometry limitations in the printing of continuous polymer-SSF parts. It was demonstrated that despite variations in the investigated angle and radii the printed teardrop samples with angles and radii greater than 30° and 5 mm respectively, exhibited print geometries which were close fit to those targeted. Overall the fit was in the range of 74-93% of the designed geometries, this was in contrast with the prints for the smallest angle and radii, for which the fit was reduced to 50%, as illustrated in Fig. 3.

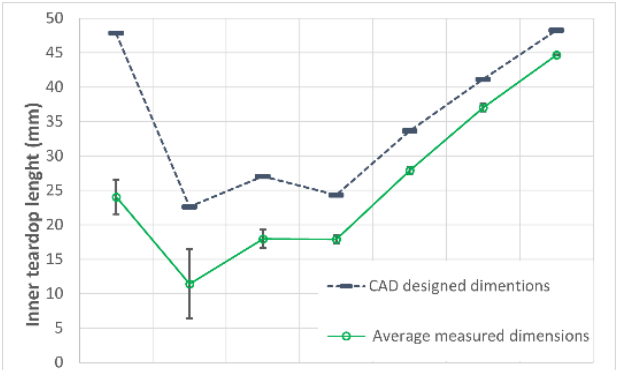

Figure 3: Teardrop geometry inner length dimensional comparison.

The width dimensions were found to increase at the end of a turn or radii, which was evaluated based on µCT scans which facilitated the measurement of the degree of distortion. The travel direction of the printer head moves in an anti-clockwise direction, as the printer head initiates the turning the SSF stays in the desired position however as it comes towards the end of the turn there it was observed to give rise to a higher level of distortion. In the case of the teardrop shapes printed at smaller angles (<5°) and radii (<4 mm); a significantly higher level of geometric distortion was observed. A further issue was the presence of fibre stringing in a number of the print geometries with lower radii semi-circles (Figure 4). This is likely to be associated with the slow solidification of the polymer as the print head changes direction, as a result, the SSF moves out of the targeted print track position. Controlling the speed at which the printer head travels around corners was found to be successful in successfully reducing the level of stringing for the smaller radii print structures.

4. Conclusion

This study investigates the geometrical limitations of 3D printing continuous 316L stainless steel fibre reinforced PLA polymer composites. Curve bend stiffness results in an increase in stiffness as the radii decrease in all materials tested.

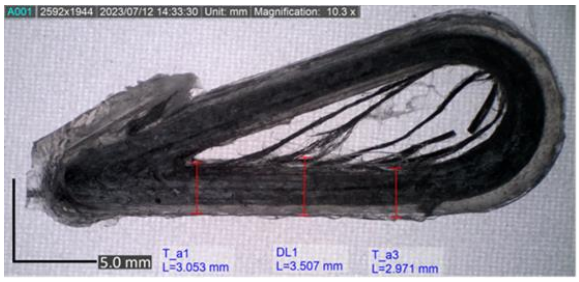

Figure 4: Teardrop with a radius of 4 mm and an angle of 20° illustrating the presence of significant levels of stringing.

The PLA-SSF showed the most significant stiffness increase at radii below 5 mm.

Teardrop-shaped components combine an angle and semi-circle dimensionally evaluated, showing repeatability in sample sets. As expected, the internal radii and acuteness of the angles degrade at smaller angles and radii. Across all samples, the effect of print height was found not to significantly influence the part geometry.

A statistical analysis has been conducted to evaluate the repeatability of the 3D printed composite samples with radii in the range from 2 to 20 mm, along with print angles between 5 to 90°. Geometric dimensions estimated based on marginal means analysis indicate a decrease in dimensional accuracy as both the print radii and angle are reduced in size. An approximately linear increase in curvature bending stiffness with a reduction in the print radii was observed.

References

[1] A. N. Dickson, H. M. Abourayana, and D. P. Dowling, "3D printing of fibre-reinforced thermoplastic composites using fused filament fabrication-A review," *Polymers (Basel).*, vol. 12, no. 10, pp. 1–20, 2020, doi: 10.3390/POLYM12102188.

[2] H. L. Tekinalp *et al.*, "Highly oriented carbon fiber-polymer composites via additive manufacturing," *Compos. Sci. Technol.*, vol. 105, pp. 144–150, 2014, doi: 10.1016/j.compscitech.2014.10.009.

[3] M. Á. Caminero, J. M. Chacón, E. García-Plaza, P. J. Núñez, J. M. Reverte, and J. P. Becar, "Additive manufacturing of PLA-based composites using fused filament fabrication: Effect of graphene nanoplatelet reinforcement on mechanical properties, dimensional accuracy and texture," *Polymers (Basel).*, vol. 11, no. 5, 2019, doi: 10.3390/polym11050799.

[4] Y. Ibrahim, "3D Printing of Continuous Wire Polymer Composite for Mechanical and Thermal Applications," YORK UNIVERSITY, 2019.

[5] M. A. Saleh, R. Kempers, and G. W. Melenka, "3D printed continuous wire polymer composites strain sensors for structural health monitoring," *Smart Mater. Struct.*, vol. 28, no. 10, 2019, doi: 10.1088/1361-665X/aafdef.

[6] A. Le Duigou, G. Chabaud, R. Matsuzaki, and M. Castro, "Tailoring the mechanical properties of 3D-printed continuous flax/PLA biocomposites by controlling the slicing parameters," *Compos. Part B Eng.*, vol. 203, no. July, p. 108474, 2020, doi: 10.1016/j.compositesb.2020.108474.

[7] ASTM, "ASTM D2344/D2344M: Standard Test Method for Short-Beam Strength of Polymer Matrix Composite Materials and Their Laminates," 2003.

[8] P. J. Hine, H. Rudolf Lusti, and A. A. Gusev, "Numerical simulation of the effects of volume fraction, aspect ratio and fibre length distribution on the elastic and thermoelastic properties of short fibre composites," *Compos. Sci. Technol.*, vol. 62, no. 10–11, pp. 1445–1453, 2002, doi: 10.1016/S0266-3538(02)00089-1.

[9] I. P. Beckman, C. Lozano, E. Freeman, and G. Riveros, "Fiber selection for reinforced additive manufacturing," *Polymers (Basel).*, vol. 13, no. 14, pp. 1–53, 2021, doi: 10.3390/polym13142231.

[10] R. Matsuzaki *et al.*, "Three-dimensional printing of continuous-fiber composites by in-nozzle impregnation," *Sci. Rep.*, vol. 6, no. December 2015, pp. 1–8, 2016, doi: 10.1038/srep23058.

[11] J. Li, Y. Durandet, X. Huang, G. Sun, and D. Ruan, "Additively manufactured fiber-reinforced composites: A review of mechanical behavior and opportunities," *J. Mater. Sci. Technol.*, vol. 119, pp. 219–244, 2022, doi: 10.1016/j.jmst.2021.11.063.

[12] L. Tack, "Bekinox® VN and Bekiflex®for Heatable Textiles," 2019.

[13] S. Oxygen *et al.*, *Inorgainc and Composite Fibers*, no. 105. Elsevier Ltd., 2018.

[14] A. Hamidi and Y. Tadesse, "Single step 3D printing of bioinspired structures via metal reinforced thermoplastic and highly stretchable elastomer," *Compos. Struct.*, vol. 210, no. March 2018, pp. 250–261, 2019, doi: 10.1016/j.compstruct.2018.11.019.

[15] D. Quan, S. Flynn, M. Artuso, N. Murphy, C. Rouge, and A. Ivanković, "Interlaminar fracture toughness of CFRPs interleaved with stainless steel fibres," *Compos. Struct.*, vol. 210, no. 1, pp. 49–56, 2019, doi: 10.1016/j.compstruct.2018.11.016.

[16] S. M. F. Kabir, K. Mathur, and A. F. M. Seyam, "A critical review on 3D printed continuous fiber-reinforced composites: History, mechanism, materials and properties," *Compos. Struct.*, vol. 232, no. June 2019, p. 111476, 2020, doi: 10.1016/j.compstruct.2019.111476.

[17] M. Gunes and I. Cayiroglu, "Mechanical Behaviour of 3D Printed Parts with Continuous Steel Wire Reinforcement," *El-Cezeri J. Sci. Eng.*, vol. 9, no. 1, pp. 276–289, 2022, doi: 10.31202/ecjse.969810.

[18] A. J. Clarke, A. Dickson, and D. P., "Fabrication and Performance of Continuous 316 Stainless Steel Fibre-Reinforced 3D-Printed PLA Composites," *Polymers (Basel).*, pp. 1–19, 2024, [Online]. Available: https://www.mdpi.com/2073-4360/16/1/63.

[19] Bekaert, "Metal fiber composite reinforcement," Zwevegem, 2018. [Online]. Available: https://www.bekaert.com/en/products/basic-materials/textile/composite-reinforcement.

[20] 3devo, “Composer 350,” 2020. [Online]. Available: https://cdn2.hubspot.net/hubfs/4595257/Product Spec Sheets/Composer-350-Specs.pdf.

[21] ISO, “ISO 14125 Fibre-reinforced plastic composites Determination of flexural properties,” Genève, 1998.